NANO LETTERS

2005
Vol. 5, No. 6
1157−1160

Nanometer Patterning with Ice

Gavin M. King,[*,†] Gregor Schürmann,[‡] Daniel Branton,[‡] and Jene A. Golovchenko[†,§]

Department of Physics, Department of Molecular and Cellular Biology, and Division of Engineering & Applied Sciences, Harvard University, Cambridge, Massachusetts 02138

Received March 3, 2005; Revised Manuscript Received April 12, 2005

ABSTRACT

Nanostructures can be patterned with focused electron or ion beams in thin, stable, conformal films of water ice grown on silicon. We use these patterns to reliably fabricate sub-20 nm wide metal lines and exceptionally well-defined, sub-10 nanometer beam-induced chemical surface transformations. We argue more generally that solid-phase condensed gases of low sublimation energy are ideal materials for nanoscale patterning, and water, quite remarkably, may be among the most useful.

Electron beam (e-beam) lithography is a powerful established method used to pattern nanometer scale structures such as single electron transistors, single molecule detectors, and nanoelectromechanical devices.[1−4] E-beam lithography typically involves applying, chemically transforming, and chemically dissolving a polymer resist.[5] The desire to decrease device size, to enhance the role of quantum mechanical device characteristics, and to pattern increasingly complex substrates requires new lithographic approaches to define nanometer scale structures. Here we demonstrate a new approach to nanoscale e-beam patterning based on the condensation and beam stimulated sublimation of water ice. Electron and ion beam stimulated sublimation of solid condensed gases has been studied in the context of cryo-electron microscopy,[6] plasma confinement,[7] and astrophysics,[8] but not, to our knowledge, for high-resolution patterning. We have discovered that frozen water, a common substance, can be used to generate nanoscale patterns of metals and potentially very useful chemical transformations on a substrate surface.

We chose this approach because it is known that electrons and very high energy ions create electronic excitations, molecular dissociations, and ionization in ice, but the consequences of these effects on nanoscale patterning have not been explored. In insulating surface layers with low sublimation energies, “Coulomb explosions” can lead to large localized agitation and ejection of surface atoms.[8] In addition, dissociation products of condensed molecular gases can be ejected after diffusion to the surface from deeper regions within the beam exposure volume.[6,9] These processes, as well as others, have been discussed,[7,10,11] but we feel it fair to conclude that the fundamental physics responsible for these observations is still obscure.

In our experiments, we deposit very thin, conformal layers of ice from water vapor onto cryogenically cooled silicon substrates in the chamber of a combined scanning electron microscope (SEM) and focused ion beam (FIB) apparatus (FEI Co., Hillsboro, Oregon). Subsequent exposure of the ice surface to focused energetic electron or gallium ion beams stimulates local removal of ice and ultimately exposes the underlying silicon substrate in whatever patterns the beams are programmed to produce. Afterward, using lower beam doses, the exposed regions can be inspected nondestructively with the SEM or FIB operating in its standard scanning imaging mode. With the sample still cold, the exposed patterned regions of the substrate can then be metallized or modified by other techniques (ion implantation, reactive ion etching, sputter deposition, etc.) in the same vacuum chamber or an adjoining one. Finally, the ice can be removed either by in situ sublimation (eliminating liquid surface tension effects) or by rinsing.

Typically, we deposit ice at a rate of ~1 nm/s using a leak valve controlled water vapor flow that is directed onto the cooled sample (Figure 1). Uniform ice coverage over ~1 mm^2 is achieved with a single needle (inner diameter ~100 μm) water vapor source held ~5 mm above the sample surface. At operating sample temperatures of 128 K the deposited ice is amorphous and sublimes at a rate of only ~0.3 monolayers/hour with a sublimation energy of 0.45 eV.[12,13] In practice, no appreciable ice sublimation is observed over several hours when working at 128 K, even with ice films <10 nm thick. The ice is promptly removed by sublimation when the sample temperature is raised to ~180 K. We have successfully patterned ice with a focused

* Corresponding author. Telephone: 303-492-7818; Fax: 303-492-5235; E-mail: gking@jilau1.colorado.edu.
† Department of Physics.
‡ Department of Molecular and Cellular Biology.
§ Division of Engineering & Applied Sciences.

10.1021/nl050405n CCC: $30.25 © 2005 American Chemical Society
Published on Web 04/29/2005

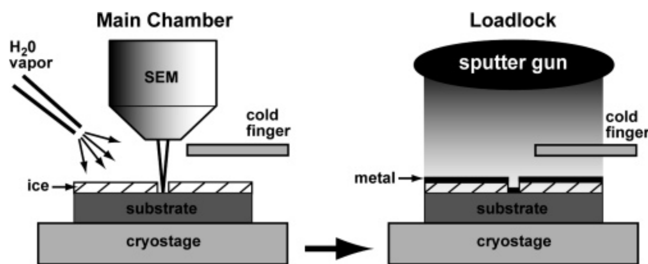

Figure 1. Schematic of the apparatus. Within the main vacuum chamber at <1 × 10^{-6} Torr, water from the vapor phase is directly condensed onto cryogenically cooled substrates, typically at 128 K. The water vapor pressure is controlled by leak valves (not shown) connected to a $MgSO_4{\cdot}7H_2O$ water vapor source. The coldfinger (located ~5 mm above the sample surface) is held at 80 K, ensuring a sufficient thermal gradient to keep unwanted species from condensing on the substrate. Ice deposition rates of ~1 nm/s are easily achieved. Substrate temperatures can be controlled to ±1 K and raised to sublime off unwanted ice. An Ar sputter gun allows for metallization in the loadlock chamber.

ion beam (30 keV Ga^+, 10 pA, diameter ~10 nm) or a focused electron beam (1−30 keV, 30−150 pA, diameter ~5 nm). All data presented here were patterned with an electron beam. After patterning, samples were transferred while cold to a connected chamber with a chromium sputter deposition source.

An in situ SEM image of a 75 nm thick layer of ice on a silicon substrate at 128 K immediately after 5 keV e-beam patterning is shown (Figure 2a). The e-beam dose used to create each of the 500 nm square patterns was increased from left to right. The sharp rise in contrast between the fourth and fifth squares indicates that a dose above 8.8 × 10^5 μC/cm^2 is required to remove the entire ice layer and expose the underlying silicon surface. An atomic force microscope (AFM) line scan and an SEM image of the same sample are shown (Figure 2b) after sputter deposition of 40 nm of Cr, removal from the vacuum chamber, and a rinse in isopropyl alcohol[14] to remove the remaining ice and its overlayer. Only the Cr that comes in contact with the patterned ice-free regions of the substrate remains after complete ice removal. No aggressive methods such as ultrasonication or mechanical scrubbing were needed to assist the liftoff. Figure 2b confirms that 5 keV e-beam doses greater than 8.8 × 10^5 μC/cm^2 are required to remove the 75 nm ice layer thickness and ensure subsequent pattern transfer to the deposited Cr. This critical dose for water ice resist is roughly 3 orders of magnitude larger than that required for a typical exposure of the polymer resist polymethyl methacrylate (PMMA). Assuming the amorphous ice layer has a density[13] 0.91 gm/cm^3, we calculate the sputter yield (i.e., H_2O molecules ejected per incident electron) $S = 0.03$ for 5 keV electrons. S decreases by over an order of magnitude as the beam energy increases from 1 to 30 keV, but it does not vary significantly with temperature between 128 and 158 K. In contrast to the relatively low electron sputter yield, we found $S \approx 12$ for 30 keV gallium ions in an FIB![15]

Figures 2c and 2d present results of varying the line dose under the same conditions as previously described for the area dose study, except with a thinner (20 nm) ice layer.

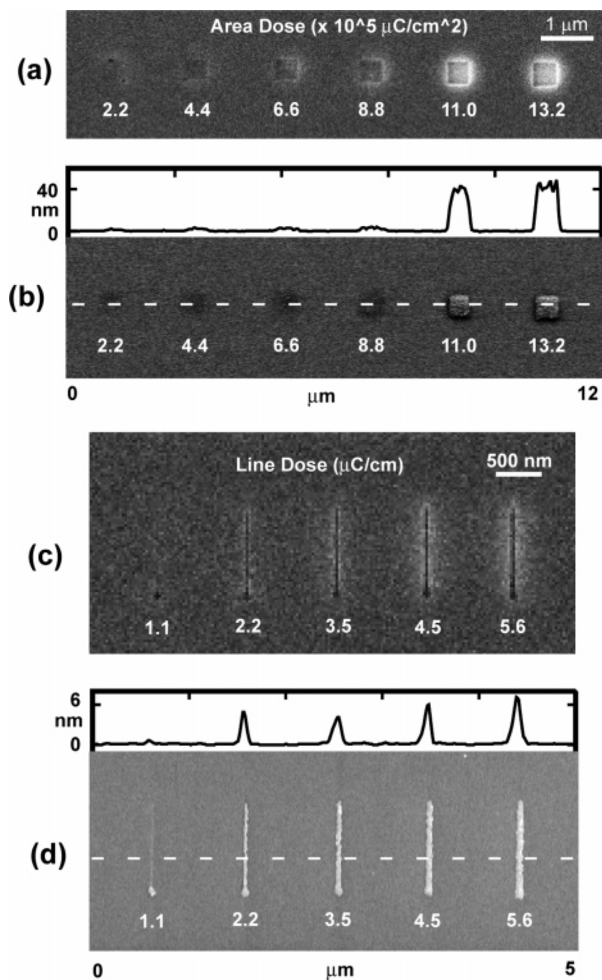

Figure 2. Patterning a silicon surface. (a) In situ cryogenic (sample $T = 128$ K) SEM image of 500 nm × 500 nm squares formed in a 75 nm thick ice layer by a 5 keV, 112 pA electron beam. The electron beam patterning dose was increased from 2.2 (left side, square barely visible) to 35.2 × 10^5 μC/cm^2 (right). (b) Room-temperature SEM image of the same sample after metallization (40 nm Cr). A topographic AFM line scan thru a region of the surface (dashed line) is shown above the SEM image. (c) In situ cryogenic SEM image of single pixel lines defined in a 20 nm thick ice layer on silicon (e-beam doses as stated). (d) Post metallization SEM and AFM line scan of the same sample.

Figure 2c is an in situ cryogenic SEM image of micron-long, single pixel lines of varying doses. Here the line dose is increased from 1.1 μC/cm (left) to 5.6 μC/cm (right). After 6 nm Cr deposition, an SEM image and an AFM line scan (Figure 2d) yield the critical line dose under these conditions of ~2.2 μC/cm. We note the patterned metal dot at the bottom end of each line allows for easy identification of underexposed regions.

The AFM scans in Figures 2b and 2d also reveal the growth of a layer of material ~ 1 nm thick in the region where the beam hit the ice even with doses too low to eject all of the ice down to the underlying substrate. We attribute this thin layer to a beam-induced surface chemical transformation that involves both the ice layer and the underlying silicon substrate because (a) the effect is observed with no metallization step; (b) the effect is specific to silicon, i.e., we see no similar growth of material on SiO_2 or Si_3N_4

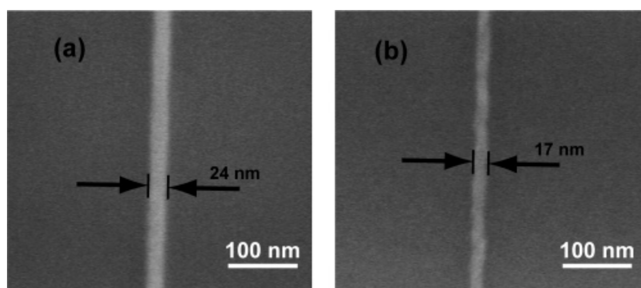

Figure 3. SEM analysis of sub-30 nm wide Cr lines on a bulk silicon substrate. Both structures were defined on 20 nm ice resist layers and subsequently metallized with 8 nm Cr. (a) 30 keV line, 4.5 μC/cm dose. (b) 20 keV line, 4.4 μC/cm dose.

substrates; (c) the material grows only to a self-terminating thickness above the silicon (111) surface; and (d) the final (self-terminated) thickness of the material scales with the amount of ice initially deposited on the silicon surface. When 5 nm of ice was deposited, subsequent e-beam exposure produced a ~0.5 nm high chemical transformation; a 75 nm ice thickness produced a 3.0 nm high structure. Further e-beam exposure did not increase the material's height. In contrast to contamination lithography,[16] observations (b) and (c) imply that we can rule out deposition of unspecified (e.g., hydrocarbon) vacuum contaminants in the chamber. Since the electron range in our experiments is larger than the ice layer thickness, observation (d) suggests that the stimulated surface chemistry required for the material growth persists only as long as the ice layer that is being removed still exists. Considering the possible species present (H_2O, its atomic or molecular fragments, silicon and hot electrons) on or near the silicon-ice interface when the beam impacts, we postulate that the thin layer of material is likely silicon oxide. This is further supported by the observation that the thin layers of material can be removed with hydrofluoric acid, leaving behind a depression in the silicon surface (Figure 4f). The electronic properties of the thin layer of material are currently under investigation.

The spatial resolution that we have achieved for ice patterned Cr lines on silicon using ~20 nm thick ice layers is shown in Figure 3 with beam exposures (a) at 30 keV and (b) at 20 keV. We note that this apparent difference in line width is potentially related to aperture alignment, astigmatism adjustment, and focus optimization steps necessary after changing the beam acceleration voltage. The narrowest dimensions of the material tentatively identified as silicon oxide (Figure 4) are, remarkably, much smaller than those obtained for Cr (Figure 3). A study of the lateral dimensions of these putative oxide structures as a function of beam energy illustrates the evident trend toward higher resolution with increasing electron beam energy. At 10 keV (Figure 4a), the structure's full width at half-maximum (fwhm) measures 18 nm. The fwhm is reduced to 14 nm at 25 keV and to 10 nm at 30 keV (Figures 4b and 4c). The measurements listed in Figure 4 are values obtained without subtracting the effective diameter of the AFM probe tip. When we account for the AFM tip effective diameter of ~5 nm (Figure 4d), the true width of these lines are of order

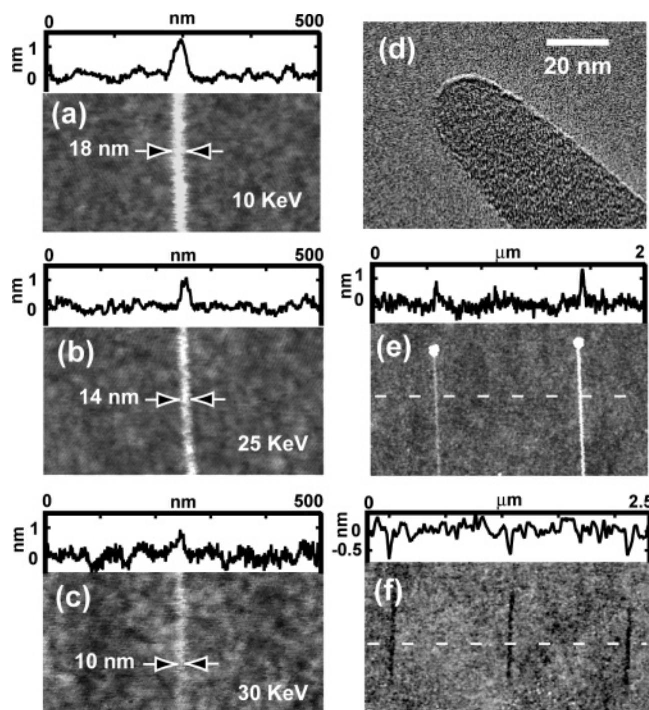

Figure 4. AFM analysis of the local electron beam induced chemical transformation of a silicon substrate. All data except panel (d) are tapping mode AFM images with associated AFM linescans. All results in (a−c) and (e) were produced with beam doses too low to eject all of the ice down to the silicon substrate. (a−c) Line width as a function of beam energy (energies as stated). (d) TEM image of the AFM tip taken after acquiring the data in (a−c). (e) Line height as a function of dose (30 keV beam). Left line, 1.5 μC/cm; right line 3.0 μC/cm. (f) Trenches are formed when raised lines similar to that shown in (e) (right line) are treated for 15 s with 48% w/w HF.

13, 9, and 5 nm for the 10, 25, and 30 keV exposures, respectively. Figure 4e shows a 2 μm × 1.5 μm AFM image of two lines defined by a 30 keV electron beam. Here we see that the 3.0 μC/cm line measures ~1.2 nm in height above the Si, while the 1.5 μC/cm line on the left is only ~0.8 nm high.

Although the "record" line widths of e-beam exposed PMMA are in the single digit nanometer range, such results were achieved with specialized higher energy beams (~100 keV) and attentive ultrasonication during resist development.[17−19] A more typical minimum line width achieved with e-beam exposed PMMA on bulk silicon substrates with commercial e-beam lithography tools is of order 30 nm.[20] To reliably achieve thinner line widths, angled depositions of metals or other materials on exposed resists are common. Our demonstrated sub-20 nm metal lines are achievable with an ice resist on bulk silicon with e-beam energies $<$30 keV and without directional deposition of metal. We speculate that proximity effects[21,22] are minimized with ice resist because the excitation of ice by backscattered electron exposure away from the point of beam incidence is not an additive process. Instead, excited ice that is not ejected from the surface can relax to its initial unexposed state.

Patterning with ices of any condensed gas is a straightforward and practical process. Ice resist does not require

spinning or baking. All processing and patterning steps can occur in a single evacuated chamber and be monitored at high resolution. The final removal of unexposed resist leaves minimal residues. Environmentally harmful solvents are not required and complete dry removal of the ice layer can be performed by in situ sublimation. Although in our current apparatus dry resist removal by sublimation after Cr metallization causes large loose Cr flakes to settle on the substrate, an inverted configuration may avoid this problem. Completely dry resist processing will be particularly useful for preparing delicate micro- and nanoelectromechanical devices on a variety of substrates, especially those exhibiting complex three-dimensional geometries.

It will be important to discover the resolution limits and to minimize the critical dose requirements by testing a wide range of beam energies, beam diameters, and other condensed gases. To avoid induced interface chemistry, rare gases are clearly called for. Alternatively, to yield desired chemical transformations, other gases can be selected to react with the substrate and produce precisely defined thickness tunnel junctions and gate insulators needed for nanoscale electronic devices. The gate insulator needed for nanoscale field effect transistors is an important example for which the material grown with water may well be suited. We anticipate that the rich and varied chemical, electronic, and mass transport properties of energetic beam stimulated solid condensed gases will provide many opportunities for discovery and innovation in connection with nanoscale patterning.

Acknowledgment. This work was supported by awards from the NSF (#DMR-0073590), DOE (#DE-FG02-01ER45922), NIH (#RO1HG02338), and Agilent Technologies. We thank the Harvard Center for Imaging and Mesoscale Structures for facilities support as well as Damon Farmer and Trygve Ristroph for assistance and discussions.

References

(1) Pashkin, Y.; Nakamura, Y.; Tsai, J. *Appl. Phys. Lett.* **2000**, *76*, 2256.
(2) Liu, K.; Avouris, Ph.; Bucchignano, J.; Martel, R.; Sun, S.; Michl, J. *Appl. Phys. Lett.* **2002**, *80*, 865.
(3) Craighead, H. *Science* **2000**, *290*, 1532.
(4) Ito, T.; Okazaki, S. *Nature* **2000**, *406*, 1027.
(5) Rai-Choudhury, P., *Handbook of Microlithography, Mircomachining, and Microfabrication*; SPIE Optical Engineering Press: London, UK, 1997.
(6) Talmon, Y.; Davis, H. T.; Scriven, L. E.; Thomas, L. E. *J. Mircoscopy* **1979**, *117*, 321.
(7) Erents, S. K.; McCraken, G. M. *J. Appl. Phys.* **1973**, *44*, 3139.
(8) Brown, W. L.; Lanzerotti, L. J.; Poate, J. M.; Augustyniak, W. M. *Phys. Rev. Lett.* **1978**, *40*, 1027.
(9) Brown, W. L.; Augustyniak, W. M.; Lanzerotti, L. J.; Johnson, R. E.; Evatt, R. *Phys. Rev. Lett.* **1980**, *45*, 1632.
(10) Ellegaard, O.; Schou, J.; Sorensen, H.; Borgesen, P. *Surf. Sci.* **1986**, *167*, 474.
(11) Watson, C. C.; Tombrello, T. A. *Radiat. Eff.* **1985**, *89*, 263.
(12) Sack, N.; Baragiola, R. *Phys. Rev. B* **1993**, *48*, 9973.
(13) Echlin, P. *Low-Temperature Microscopy and Analysis*; Plenum Press: New York, 1992.
(14) Liquid water also works for this purpose. Techniques to remove the Cr overlayer in situ have not been explored.
(15) Conventional organic polymer resists are 10−100 times more sensitive to ion irradiation than to electron exposure (Wolf, S. and Tauber, R., *Silicon Processing for the VLSI Era*; Lattice Press: Sunset Beach, California, 1986). Based on this measured ion sputter yield we estimate the effectiveness of ice resist as an ion implantation mask: ∼4 nm of ice is required per monolayer of implanted ions (30 keV Ga).
(16) Broers, A.; Hoole, A.; Ryan, J. *Microelectron. Eng.* **1996**, *32*, 131.
(17) Vieu, C.; Carcenac, F.; Pepin, A.; Chen, Y.; Mejias, M.; Lebib, A.; Manin-Ferlazzo, L.; Couraud, L.; Launois, H. *Appl. Surf. Sci.* **2000**, *164*, 111.
(18) Chen, W.; Ahmed, H. *Appl. Phys. Lett.* **1993**, *62*, 1499.
(19) Craighead, H. G.; Howard, R. E.; Jackel, L. D.; Mankiewich, P. M. *Appl. Phys. Lett.* **1983**, 42, 38.
(20) Raith 150 Ultrahigh-resolution E-beam lithography and metrology tool, Product data sheet: minimum feature size = 30 nm. Raith GmbH, Dortmund (Germany).
(21) Chang, T. H. P. *J. Vac. Sci. Technol.* **1975**, *12*, 1271.
(22) Chen, W.; Ahmed, H. *Adv. Imag. Elect. Phys.* **1998**, *102*, 87.

NL050405N